2005-01-2456

Stick-Slip Behavior of Torque Converter Clutch

Chengwu Duan and Rajendra Singh
Acoustics and Dynamics Laboratory
Center for Automotive Research
The Ohio State University

ABSTRACT

The chief objective of this paper is to study the non-linear behavior of torque converter clutch within the context of an automotive drivetrain. An analytical procedure to determine the pure stick to stick-slip motions is developed based on the linear system analysis. This procedure can efficiently and accurately identify the frequency ranges where linear or non-linear studies are needed. Stick-slip behavior can be clearly observed as a result of the engine torque irregularity and nonlinear friction characteristics. In particular, the effect of the friction disc inertia is studied. Both analytical and numerical results show that this inertia significantly affects the system dynamics. Our predictions compare well with prior measurements on a passive vibration absorber experiment.

INTRODUCTION

Friction elements are commonly found in many mechanical and structural systems. For example, consider the automotive torque converter clutch (TCC) sub-system that consists of a fluid torque converter and in parallel a mechanical wet friction clutch as shown in Figure 1a. When the engine speed Ω_e is low, the wet friction clutch is fully disengaged and only the fluid torque converter path is operational. The pump drives the turbine with a torque generated by a change in the momentum of the fluid. Torque amplification is allowed and a smooth shift or transition is allowed [1]. At a higher speed, the mechanical clutch is fully engaged and the fluid path is no longer in effect. Under this condition, the transmission is directly driven by the engine. The energy dissipated within the torque converter is minimized to enhance the fuel efficiency. Over the mid-speed range, the TCC is partially engaged and both the wet friction clutch and the fluid torque converter transmits torque [2-3]. The TCC is designed to transmit very high torque loads and to suppress a large slip between engine and transmission to avoid overheating. However, the stick-slip phenomenon often takes place within the TCC as a consequence of significant torque pulsations from the engine and nonlinear friction characteristics [3-5]. For example, “slip hunting” or stick-slip problem is found in the controlled (minimum) slip TCC [4]. The resulting stick-slip could excite several vibration problems in the driveline system, thereby deteriorating the vehicle ride quality. Although some state-of-the-art applications use the controlled slip technology, stick-slip phenomenon could still take place because of engine torque pulsations, friction characteristics and run outs in the contact surface etc. In fact, to the best of authors' knowledge, avoidance of stick-slip is still a technical challenge that might prevent more wide spread usage of control slip concepts. To study the dynamic effects of stick-slip within a driveline system with TCC, we will study the non-linear dynamic characteristics of a three-degree of freedom (3DOF) semi-definite torsional system with a friction-controlled path as shown in Figure 1b.

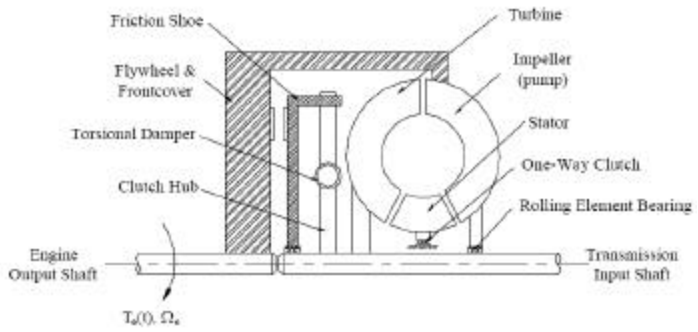

a)

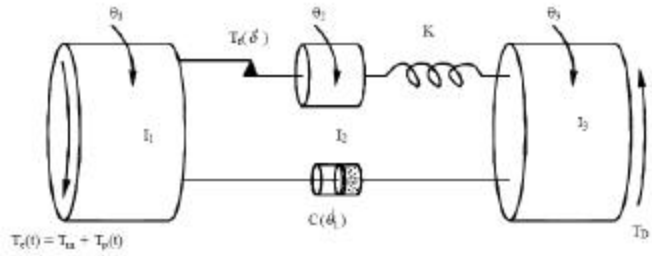

b)

Figure 1 Problem Formulation. a) Schematic of a typical automotive torque converter and wet friction clutch (TCC). b) 3DOF semi-definite torsional model of an automotive driveline system.

TORSIONAL SYSTEM WITH FRICTION PATH

The driveline system can be reasonably represented by a 3DOF semi-definite system with focus on the TCC sub-system. This is conceptually similar to the manual transmission formulation employed by Padmanabhan and Singh [6] to study gear rattle and to the automatic transmission model utilized by Yamada and Ando [7] to examine clutch judder. As shown in Figure 1b, I_1 represents the combined torsional inertia of flywheel, front cover and impeller; I_2 is the inertia of friction disc assembly (secondary inertia) and I_3 is the reflected torsional inertia of the rest of the driveline system. The governing equations for this 3DOF semi-definite system with a non-linear friction path as given by T_f are:

$$I_1\ddot{q}_1 + C(\dot{q}_1)(\dot{q}_1 - \dot{q}_3) + T_f(d_1,\dot{d}_1) = T_e(t) \quad (1a)$$

$$I_2\ddot{q}_2 + K(q_2 - q_3) - T_f(d_1,\dot{d}_1) = 0 \quad (1b)$$

$$I_3\ddot{q}_3 - C(\dot{q}_1)(\dot{q}_1 - \dot{q}_3) - K(q_2 - q_3) = -T_D(t) \quad (1c)$$

Here, q_1, q_2 and q_3 are absolute angular displacements, $C(\dot{q}_1)$ is the engine speed-dependent viscous damping term which represents the fluid path, K is the linear torsional stiffness, $T_e(t)$ is the engine torque (including mean and dynamic terms) and $T_D(t)$ is the drag load as experienced by the driveline. Further, in Equation (1), $T_f(\dot{d}_1)$ is a function of the relative velocity $\dot{d}_1 = \dot{q}_1 - \dot{q}_2$ across the friction interface. When the relative motions are of interest, the system can be further reduced to the following 2DOF definite system, where $d_2 = q_2 - q_3$ and $\dot{d}_2 = \dot{q}_2 - \dot{q}_3$:

$$I_2\ddot{d}_1 + C(\dot{q}_1)\frac{I_2}{I_1}(\dot{d}_1 + \dot{d}_2) - Kd_2 + \frac{I_1 + I_2}{I_1}T_f(d_1,\dot{d}_1) = \frac{I_2}{I_1}T_e(t) \quad (2a)$$

$$I_2\ddot{d}_2 + C(\dot{q}_1)\frac{I_2}{I_3}(\dot{d}_1 + \dot{d}_2) + \frac{I_2 + I_3}{I_3}Kd_2 - T_f(d_1,\dot{d}_1) = \frac{I_2}{I_3}T_D(t) \quad (2b)$$

Table 1 lists typical values of parameters and excitation used for simulation studies.

SCOPE AND ASSUMPTIONS

The engine torque $T_e(t)$ is composed of mean T_m and pulsating $T_p(t)$ components. In this study, only the dominant frequency component is considered for the sake of simplicity. The drag load $T_D(t)$ consists of wheel rolling resistance and aerodynamic drag. It is further assumed that the vehicle speed is constant and the vehicle drag and the mean engine load are balanced, $T_m = T_D$.

Even when the TCC is partially engaged, most of the torque is transmitted by the mechanical path during the steady-state response when the slip speed is relatively small [3]. Thus the driveline system dynamics is assumed to be mostly affected by the mechanical stick-slip motions. In this case, the fluid path term $C(\dot{q}_1)$ is further approximated by a linear viscous damping C. In a real system, C could be around 1.0 N-m-s/rad [1].

Parameters and Excitation	Value(s)
Inertias (kg-m^2)	I_1 = 0.20, I_2 = 0.02, I_3 = 6.6
Viscous Damping (Nm-rad/s)	C = 1.0
Stiffness (Nm/rad)	K = 1010
Saturation Friction Torque (Nm)	T_{sf} = 350
Excitation Amplitude (Nm)	T_m = 100, T_p = 250

Table 1 Values of parameter and excitation amplitude used for simulating the 3DOF system of Figure 1b.

COMPUTATION OF STICK TO SLIP BOUNDARIES BASED ON LINEAR SYSTEM MODELS

Under the condition of a high friction torque T_{sf}, a closer observation would find that the friction interface is purely under the stick condition over some frequencies. A linear system analysis is first conducted to find this frequency regime. In this case, I_1 and I_2 move together as a single rigid body as shown in Figure 2 and the 3DOF semi-definite system is reduced to a 2DOF semi-definite system with equations as:

$$(I_1 + I_2)\ddot{q}_1 + C(\dot{q}_1 - \dot{q}_3) + K(q_1 - q_3) = T_e \quad (3a)$$

$$I_3\ddot{q}_3 - C(\dot{q}_1 - \dot{q}_3) - K(q_1 - q_3) = -T_D \quad (3b)$$

Reducing this linear system further into SDOF definite system, the governing equation is given as follows where the sinusoidal excitation (at w with amplitude T_{eq}) under a mean load T_m is applied:

$$I_{eq}\ddot{d} + C\dot{d} + Kd = T_m + T_{eq}\sin(wt) \quad (4)$$

Where, $d = q_1 - q_3 = q_2 - q_3$, $I_{eq} = I_3(I_1 + I_2)/(I_1 + I_2 + I_3)$ and $T_{eq} = T_p I_3/(I_1 + I_2 + I_3)$. The analytical solution for the steady

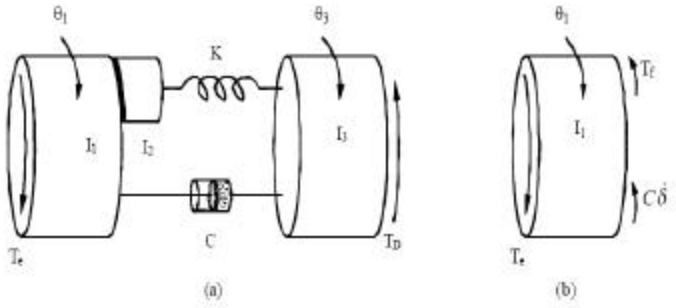

Figure 2 Resulting torsional systems. (a) Pure stick condition; (b) Free body diagram for I_1 under pure stick condition.

state oscillatory motions (d and $\dot{d}$) is as follows where $y = \tan^{-1}[Cw/(K - I_{eq}w^2)]$ is the phase lag.

$$d(t) = \frac{T_m}{K} + \frac{T_{eq}}{\sqrt{(K - I_{eq}w^2)^2 + (Cw)^2}} \sin(wt - y) \quad (5a)$$

$$\dot{d}(t) = \frac{T_{eq}w}{\sqrt{(K - I_{eq}w^2)^2 + (Cw)^2}} \cos(wt - y) \quad (5b)$$

As seen from the free body diagram of Figure 2b, the following relationship holds under the pure stick condition:

$$T_e(t) - I_1\ddot{q}_1(t) - C\dot{d}(t) = T_f(t) \quad (6a)$$

Then the transition condition from stick to slip is:

$$\left|T_e(t) - I_1\ddot{q}_1(t) - C\dot{d}(t)\right| > T_{sf} \quad (6b)$$

From equation (3), we find the breakaway condition as:

$$\left|\frac{I_2}{I_1 + I_2}T_e(t) - \frac{I_2}{I_1 + I_2}C\dot{d}(t) + \frac{I_1}{I_1 + I_2}Kd(t)\right| > T_{sf} \quad (7)$$

As evident from this analysis, the stick to slip boundary is determined by system parameters of Table 1. As shown in Figure 3a, the upper threshold frequency drops as the secondary inertia I_2 is increased. Depending on the friction saturation torque, the pure stick regime exists at lower frequencies as shown in Figure 3b. The excitation amplitude yields an opposite trend in Figure 3c where the pure stick regime occurs at a lower excitation torque. This analysis can also be applied to other physical systems where a friction element is present. The stick-slip transition could be quickly located and the entire simulation process would become more time efficient.

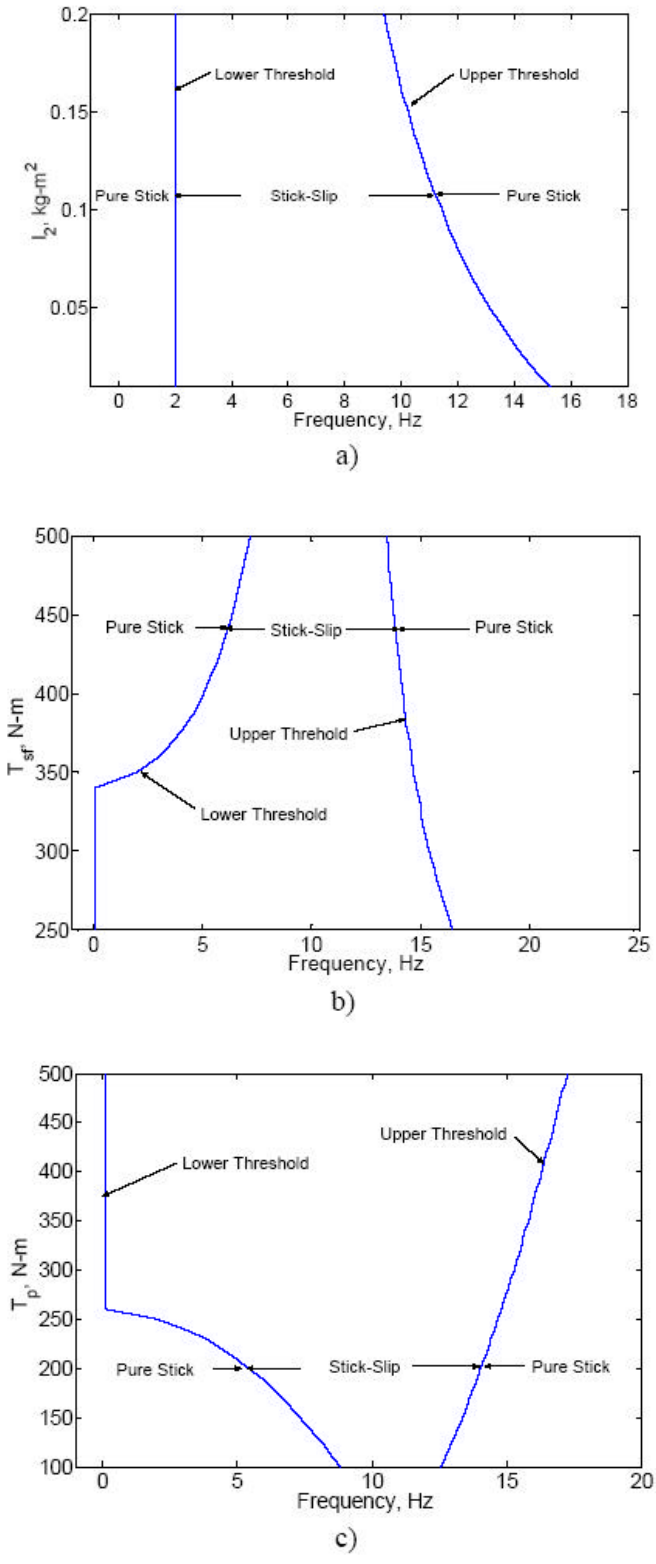

Figure 3 Stick-slip boundaries based on linear system analysis. (a) Variation with respect to I_2; (b) Variation with respect to T_{sf}; (c) Variation with respect to excitation amplitude of T_p.

NON-LINEAR SYSTEM SOLUTION

When the frictional interface experiences stick-slip motions, non-linear methods are applied to obtain the responses. The first scheme is a discontinuous friction formulation. Three states are defined according to friction interface dynamics: positive slip, negative slip and stick. In the case of positive slip, the system can be described by the following governing equation:

$$I_2\ddot{d}_1 + C\frac{I_2}{I_1}(\dot{d}_1 + \dot{d}_2) - Kd_2 + \frac{I_1 + I_2}{I_1}T_{sf} = \frac{I_2}{I_1}T_e(t) \qquad (8a)$$

$$I_2\ddot{d}_2 + C\frac{I_2}{I_3}(\dot{d}_1 + \dot{d}_2) + \frac{I_2 + I_3}{I_3}Kd_2 - T_{sf} = \frac{I_2}{I_3}T_D \qquad (8b)$$

In a similar manner, the system under the negative slip state can be illustrated by changing the sign associated with T_{sf} terms in (8). Under stick state, equation (4) can be used. Now we can solve the responses for three states and then assemble the solutions by matching continuity conditions of force and velocity across the frictional interface. This method yields an "exact" solution but much time is consumed during the iterative matching process.

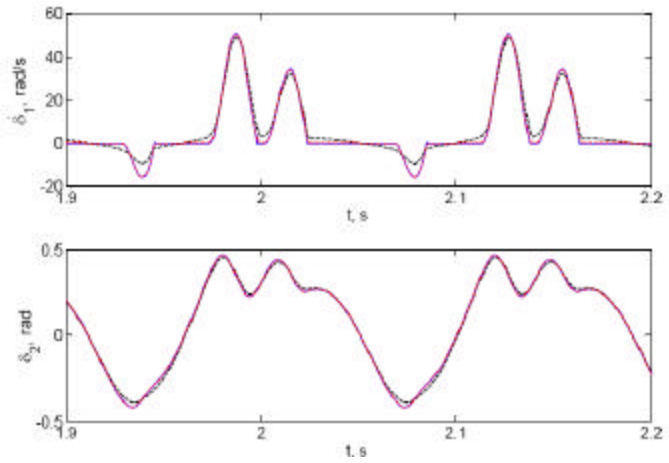

Figure 4 Comparison of two friction path models in terms of time histories. ___, discontinuous friction model; - - -, smoothened model with σ = 0.5; - · -, smoothened model with σ = 10^2.

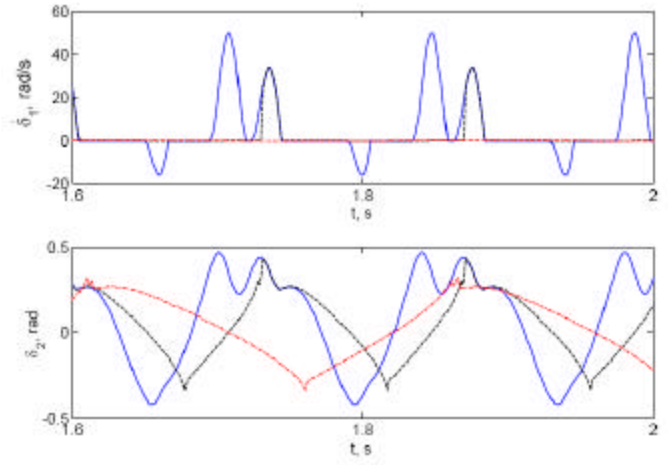

Figure 5 Comparison of two friction path models in terms of time histories. ___, discontinuous model; - - -, smoothened model with σ = 10^3; - · -, smoothened model with σ = 2×10^3

The second solution is a smoothened friction formulation where the discontinuous friction law is conditioned via a smoothening function.

$$T_f(\dot{d}_1) = T_{sf}\tanh(s\dot{d}_1) \qquad (9)$$

Here, s is a smoothening factor. Substitute (9) to (2) and now the non-linear response can be calculated by direct numerical integration employing an explicit Runge-Kutta routine [8]. Results have shown that this method can calculate the motions relatively quick. However, artificial uncertainty has been introduced by the smoothening factor. For instance, a lower s value gives a smoother torque curve and faster convergence is achieved in numerical integration. Conversely, a higher s value can produce a Coulomb-like $T_f(\dot{d})$ curve. But too abrupt transition(s) would introduce numerical stiffness issues. Illustrative results are given in Figures 4 and 5. When s is 100, the calculated system response is almost identical to the one found with the discontinuous model. When s is low such as 0.5, no pure stick regime is found in $\dot{d}_1(t)$ of Figure 4. The friction torque undergoes a relatively smooth transition but the calculated response of $d_2(t)$ shows some differences. On the other hand, when s is over 1000, the time domain responses of Figure 5 are incorrect. Therefore, the dynamic response is very sensitive to the judicious choice of s. However, the best value of s usually is not known *a priori* and it could depend on system parameters. Consequently, the discontinuous friction model should be used as benchmark if successfully implemented.

BI-LINEAR FRICTION SYSTEM ANALYSIS

Many researchers [9-13] have studied the conventional bi-linear friction system (Figure 6) that assumes a massless link between the spring and the friction elements, i.e. $I_2 = 0$. Similar to the physical system of Figure 1b, equations for bi-linear friction system can be given on a state-by-state basis. First, for the positive slip state, the equation is:

$$\frac{I_1 I_3}{I_1 + I_3}\ddot{d}_1 + C\dot{d}_1 + T_{sf} = \frac{I_3}{I_1 + I_3}T_e + \frac{I_1}{I_1 + I_3}T_D \qquad (10)$$

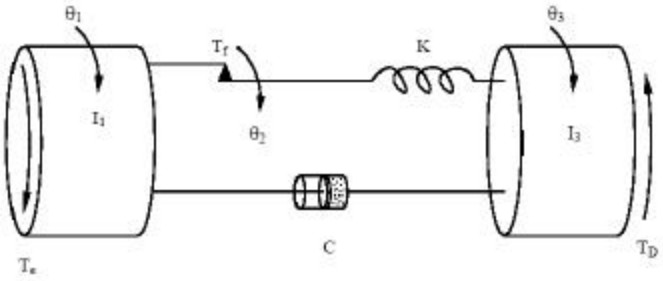

Figure 6 Schematic of the bi-linear torsional system (with $I_2 \to 0$). Here, T_f represents a friction path.

Since no inertial body exists between the friction and spring elements, the torque acting on the torsional spring is constant (T_{sf}). Consequently, the value of d_2 remains T_{sf}/K and $\dot{d}_2$ is zero. Second, for the case of negative slip, the equation is rewritten by changing the sign of T_{sf} in (10)

Further, the equation for the pure stick state is given by:

$$\frac{I_1 I_3}{I_1 + I_3}\ddot{d}_2 + C\dot{d}_2 + Kd_2 = T_m + \frac{I_3}{I_1 + I_3}T_p(t) \qquad (11)$$

The system of Figure 1b can now be compared with that of Figure 6. Both show the second order system behavior under the stick condition. However, under the positive or negative slip state condition, the bi-linear friction system exhibits a first order system behavior while the model with I_2 follows a second order system. For this reason, some key differences between these two systems are expected, as explored in the subsequent section.

EFFECT OF THE SECONDARY INERTIA

A comparison of equations (4) and (11) shows that the effect of the secondary inertia I_2 could be negligible under the pure stick condition in the presence of a very small I_2. For this reason, we examine the effect of I_2 in the positive or negative slip state. First, consider a conventional bi-linear friction system undergoes transition from pure stick to positive slip state. Equation (12a) describes the governing equation for the system in the pure positive slipping motion. A phase term j_c is intentionally included in the excitation torque expression since the absolute transition time t_c may not be integer multiplier of the excitation period (P). Consequently, given $T_D = T_m$, equation (10) has to be rewritten as follows where $I_{1e} = I_1 I_3/(I_1 + I_3)$ and $T_{pe} = T_p I_3/(I_1 + I_3)$.

$$I_{1e}\ddot{d}_1 + C\dot{d}_1 = (T_m - T_{sf}) + T_{pe}\sin(wt + j_c). \qquad (12a)$$

$$P = \frac{2p}{w}, \qquad j_c = \left[t_c - \text{int}\left(\frac{t_c}{P}\right)\right]w. \qquad (12b\text{-}c)$$

The operator $\text{int}()$ yields the integer portion of a fraction number. Now, the general solution of $\dot{d}_1(t)$ is a combination of homogeneous and particular solutions as follows:

$$\dot{d}_1(t) = Ae^{-\frac{C}{I_{1e}}t} + \left[a_0 + a_1\cos(wt) + a_2\sin(wt)\right] \qquad (13)$$

The coefficients (a_0, a_1 and a_2) are obtained by matching the particular solutions on both sides of (13) as follows:

$$a_0 = \frac{T_m - T_{sf}}{C}, \qquad a_1 = T_{pe}\frac{C\sin j_c - I_{1e}w\cos j_c}{I_{1e}^2 w^2 + C^2},$$

$$a_2 = T_{pe}\frac{C\cos j_c + I_{1e}w\sin j_c}{I_{1e}^2 w^2 + C^2}. \qquad (14a\text{-}c)$$

The constant A needs to be determined by the initial condition. As noted from the previous section, when the frictional interface experiences a transition from pure stick to positive slip motion, d_2 reaches the maximum amplitude T_{sf}/K and retains this value during the entire subsequent pure slip state. To satisfy this dynamic condition, $\dot{d}_2$ experiences a finite jump from a certain value V at the end of pure stick state to 0 at the start of pure slip state. For this reason, a corresponding finite jump from 0 to V must occur in $\dot{d}_1$ to satisfy the following continuity condition when we reset the transition time as 0.

$$(\dot{q}_1 - \dot{q}_3)\Big|_{t=t_{0-}} = (\dot{q}_1 - \dot{q}_3)\Big|_{t=t_{0+}} \qquad (15)$$

Thus, the initial condition of $\dot{d}_1(t)$ is determined, $\dot{d}_1(0) = V$. Use this to find A of (13) and write the complete response of $\dot{d}_1(t)$ as follows:

$$\dot{d}_1(t) = (V - a_0 - a_1)e^{-\frac{C}{I_1}t} + a_0 + a_1\cos(wt) + a_2\sin(wt) \quad (16)$$

Observe that the oscillatory terms associated with a_1 and a_2 only contains only one frequency (w).

Next, the 3DOF system ($I_2 \neq 0$) is considered. Assume a very small I_2, say $I_2/I_1 = 0.005\sim0.01$. Equations (8) are approximated as follows:

$$I_2\ddot{d}_1 + C\frac{I_2}{I_1}(\dot{d}_1 + \dot{d}_2) - Kd_2 + T_{sf} = 0 \quad (17a)$$

$$I_2\ddot{d}_2 + C\frac{I_2}{I_3}(\dot{d}_1 + \dot{d}_2) + Kd_2 - T_{sf} = 0 \quad (17b)$$

Since the excitation torque is neglected due to $I_1 >> I_2$, the phase lag j_c term that accurately represents the excitation as discussed in the previous section is no longer an issue here. Further, equation (17a) is further simplified given $I_3 >> I_2$; refer to Table 1 for typical parameters.

$$I_2\ddot{d}_2 + C\frac{I_2}{I_3}\dot{d}_2 + Kd_2 - T_{sf} = 0 \quad (18)$$

Equation (18) can be conveniently solved and the approximated solution for d_2 is obtained where $w_n \cong \sqrt{K/I_2}$.

$$d_2(t) = b_0 + b_1 e^{-\frac{C}{2I_3}t}\cos(w_n t) + b_2 e^{-\frac{C}{2I_3}t}\sin(w_n t) \quad (19)$$

The initial conditions for $d_2(t)$ at the transition time are $d_2(0) = T_{sf}/K$ and $\dot{d}_2(0) = V$. Since I_2 has a very small but non-zero value, its absolute velocity or momentum can only be changed by an infinite large impulsive force within an infinitesimal time span that is physically impossible. Consequently, no jump could take place in $\dot{d}_2(t)$ unlike the one exhibited by bi-linear friction system. Instead, $\dot{d}_2(t)$ is a smooth function of time.

$$\dot{d}_2(t) = \frac{T_{sf}}{K} + \frac{V}{w_n}e^{-\frac{C}{2I_3}t}\sin(w_n t) \quad (20)$$

As noted, $d_2(t)$ oscillates around the mean value T_{sf}/K unlike the bi-linear friction system. Further, since I_2 is very small, the oscillation frequency (w_n) is very high. To conveniently obtain an approximate analytical solution for $\dot{d}_1(t)$, we neglect the damping term in equation (18) and substitute the relation in equation (17), and obtain the following governing equation.

$$I_2(\ddot{d}_1 + \ddot{d}_2) + C\frac{I_2}{I_1}(\dot{d}_1 + \dot{d}_2) = 0 \quad (21)$$

Where the initial condition is defined as $(\dot{d}_1 + \dot{d}_2)\big|_{t=0} = \dot{d}_2\big|_{t=0} = V$. Finally, the approximate analytical solution of $\dot{d}_1(t)$ is obtained.

$$\dot{d}_1(t) = V\left[e^{-\frac{C}{I_1}t} - e^{-\frac{C}{2I_3}t}\cos(w_n t)\right] \quad (22)$$

Similar to $d_2(t)$, a very high frequency oscillatory term is found in $\dot{d}_1(t)$ along with an exponentially decaying term. Further, it is noted that the above analyses could be applied to the negative slip state in a similar manner.

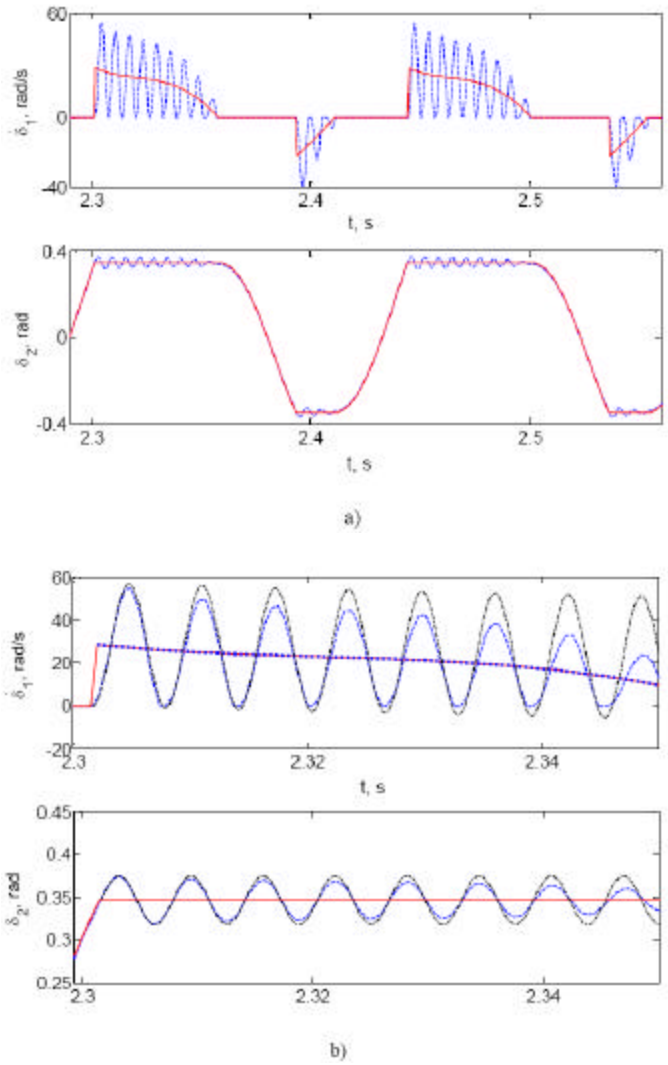

Figure 7 Effect of I_2 on time histories. a) Numerical solutions: ___, I_2/I_1 = 0; - - -, I_2/I_1 = 0.005. b) Comparison between numerical and analytical solution during the positive slip state: ___, numerical solution given I_2/I_1 = 0; …, analytical solution given I_2/I_1 = 0; - - -, numerical solution given I_2/I_1 = 0.005; - · -, analytical solution given I_2/I_1 = 0.005.

Figures 7 compare the results corresponding to $I_2 / I_1 \neq 0$ (system of Figure 1b) and 0 (the conventional bi-linear system of Figure 6) cases. As expected, the motion differences under the pure stick condition ($\dot{d}_1 = 0$) are minimal since I_2 is very small compared to I_1 as shown in Figures 7a. Under the slip condition ($\dot{d}_1 > 0$), the difference is however noticeable. As response makes a transition from stick to slip, $\dot{d}_1$ of the bi-linear system (with $I_2 = 0$) shows a finite jump from zero to the value of $\dot{d}_2$ at the end of previous stick state and then it goes back to zero (stick) gradually. The values of d_2 are bounded within $\pm T_{sf} / K$. Overall, the response resembles the "relaxation oscillation" [14], i.e. the potential energy is incrementally stored in the spring during the pure stick state and then suddenly released during the stick to slip transition. However, our response does not quite follow the classical "relaxation oscillation" behavior since the underlying mechanism is essentially different. According to Den Hartog [15] and Andronov et. al. [16], the "relaxation oscillation" is self-excited due to the existence of negative damping, such as the friction element with a negative slope in an autonomous system. In contrast, the response displayed by our bi-linear friction system is a result of the external torque excitation in the presence of a friction term and as such no negative damping element is present. In fact, Minorsky [17] has suggested that generic quasi-discontinuous motions may describe two kinds of oscillations: (i) relaxation oscillations and (ii) impulse-excited oscillations that are induced by an external impulsive cause. Although our response cannot be classified as impulse-excited oscillations either, we would still categorize as a quasi-discontinuous oscillations. Further research is needed to explore this issue.

On the contrary, the system response with a non-zero I_2 is, however, quite different. With the existence of a secondary inertia, an abrupt change or finite jump in $\dot{d}_1$ at the transition point does not occur. But the slip velocity is much higher than the one in the bi-linear friction case. With the initial conditions and absolute transition time provided by numerical solution, approximate analytical solutions for $\dot{d}_1$ and d_2 are also obtained by using equations (16) and (19), and (22) respectively. Comparative results in Figures 7b show a good agreement between the approximate analytical solutions and exact numerical solutions. Some minor difference for the $I_2 \neq 0$ case could be due to inadequate damping in the approximate model. The reason that $\dot{d}_1(t)$ just decreases gradually with time without active oscillations with bi-linear friction system is that the oscillatory term in equation (16) is at excitation frequency w and this frequency is very low compared to $w_n = \sqrt{K / I_2}$ since a very small value of I_2 is used. Also, only period-one motions are observed.

More time histories plots are presented in Figure 8. It is seen that an increase in I_2 decreases the severity of the interfacial stick-slip. At the excitation frequency of 7 Hz, the negative slip disappears when $I_2 = 0.4 I_1$. As stated previously in the stick to slip boundary analysis, there exists a specific value of I_2 that would induce a purely stick regime and thus $d_2(t)$ is governed strictly by a linear system.

A more comprehensive understanding on the effect of I_2 could be achieved by constructing the non-linear frequency response characteristics. Dynamic responses

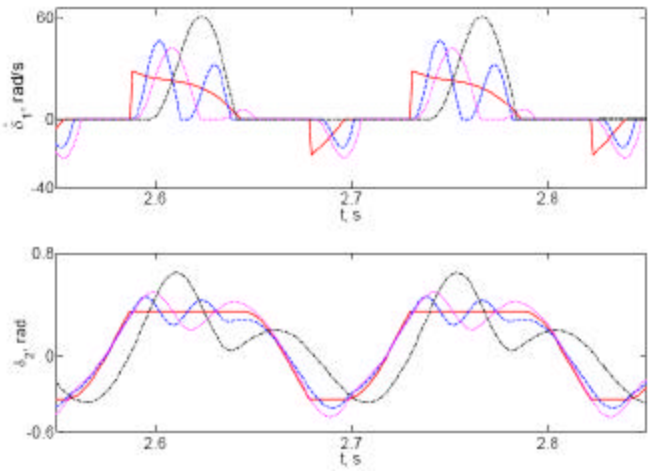

Figure 8 Effect of I_2 on time histories: ___, I_2/I_1 = 0; - - -, I_2/I_1 =0.1; . . ., I_2/I_1 = 0.2;- · -, I_2/I_1 = 0.4.

may be quantified by taking the maximum (max) and minimum (min) values from the calculated time history at each excitation frequency. Figure 9a shows the response maps in terms of $d_{2\max}$ and $d_{2\min}$ values. Stick-slip boundaries as found earlier by the linear system theory are also plotted. Since there is no spring in parallel with the friction element, the relative displacement $d_1(t)$ may grow up to a very large value under the influence of a mean load T_m. Thus, no physical meaning could be associated with max or min values of the steady state $d_1(t)$. Instead, the non-linear frequency response of relative displacement d_2 is of chief interest here. Also, we find the root-mean-square (rms) values from the calculated time histories, again at each excitation frequency as shown in Figure 9b.

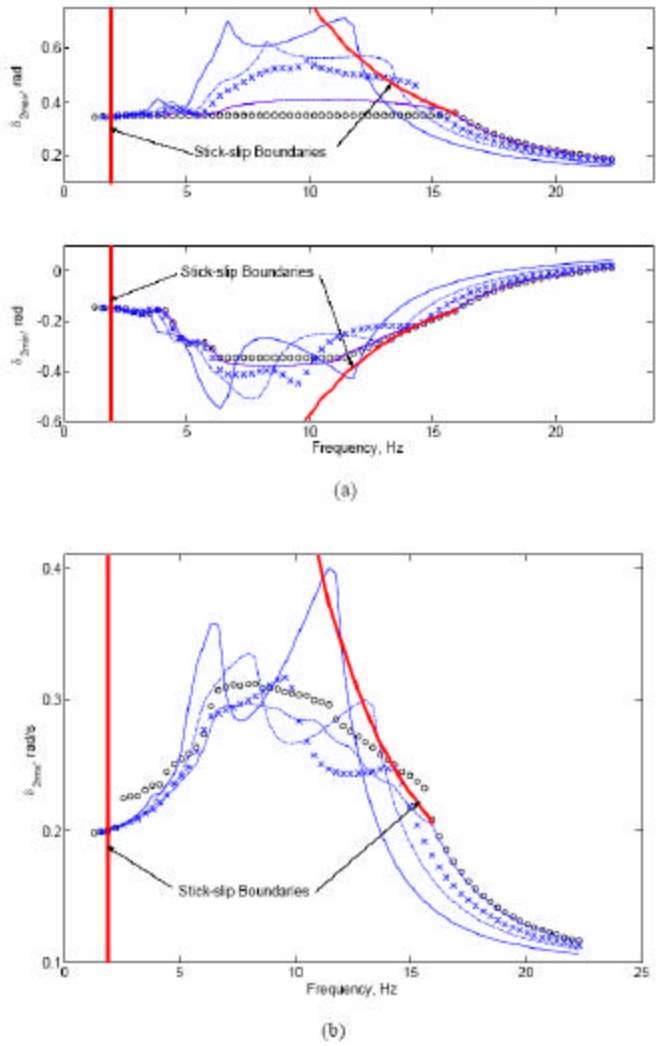

Figure 9 Effect of I_2 on responses over a range of excitation frequencies. (a) Maximum and minimum responses: ooo, I_2/I_1 = 0; - - -, I_2/I_1 = 0.01; xxx, I_2/I_1 = 0.1; - · -, I_2/I_1 = 0.2; ___, I_2/I_1 = 0.4; (b) rms responses: ooo, I_2/I_1 = 0; - - -, I_2/I_1 = 0.01; xxx, I_2/I_1 = 0.1; - · -, I_2/I_1 = 0.2; ___, I_2/I_1 = 0.4.

As expected from the stick to slip boundary analysis, an increase in the value of I_2 narrows the stick-slip regime. It is also clearly observed in Figure 9a that as I_2 increases, the max to min value of d_2 over the pure stick (linear) regime is lowered. However, the values over the stick-slip regime go up. Unlike the bi-linear hysteresis case where the peak amplitude is constant ($d_2 = T_{sf}/K$), the amplitudes with non-zero I_2 exhibit "resonance-like" curves in Figure 9. Such resonances are dictated by a combination of 2 states: 2DOF and 3DOF system responses. A comparison of the rms maps in Figure 9b shows similar effects of I_2.

EXPERIMENTAL VALIDATION

Next we compare our method with one benchmark example as available in the literature: Hartung et. al.'s passive vibration absorber analyses [18]. Physical model of their study could be conceptually described by the sub-sets of Figure 1b since the friction is the only non-linear element in two degree of freedom systems.

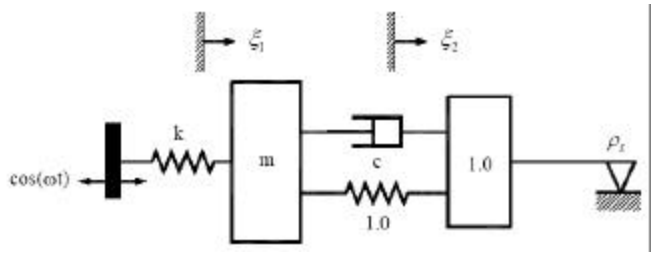

Figure 10 Hartung et. al.'s passive vibration absorber model [18]

The governing equations for the system shown in Figure 10 are as follows using their nomenclature.

$$m\ddot{x}_1 + c\dot{x}_1 - c\dot{x}_2 + (1+k)x_1 - x_2 = k\cos(wt) \qquad (23)$$

$$\dot{x}_2 - c\dot{x}_1 + c\dot{x}_2 - x_1 + x_2 = -r_s g(\dot{x}_2) \qquad (24)$$

Aside from numerical simulation based on the discontinuous friction model, they also conducted an experimental study and investigated the effect of friction force amplitude r_s. Selected measured frequency response curves under three friction forces are extracted from [18] and illustrated in Figure 11. First we predict the stick to slip boundaries using the linear system procedure proposed earlier. Second, we employ the discontinuous and smoothened friction models. Our simulation results, as shown in Figure 12, show a very good match with measured curve of Figure 11 even when the smoothened friction model is chosen. As the friction force increases, the stick-slip motion is suppressed in Figure 12. The stick-slip motion virtually disappears in Figure 12c when the friction force increases to a certain value and finally the system is degenerated into a linear single degree of freedom system. Although Hartung et. al.'s experiment [18] showed that the friction-induced characteristics depend on normal or friction force amplitude, our comparisons reveal that the even simplest friction model could still be used to qualitatively assess the non-linear responses or quantitatively estimate the stick-slip boundaries. Thus, we validate our linear and non-linear methods. With the validation from benchmark experimental work, the presented analytical results can be applied to understand the real life clutch application.

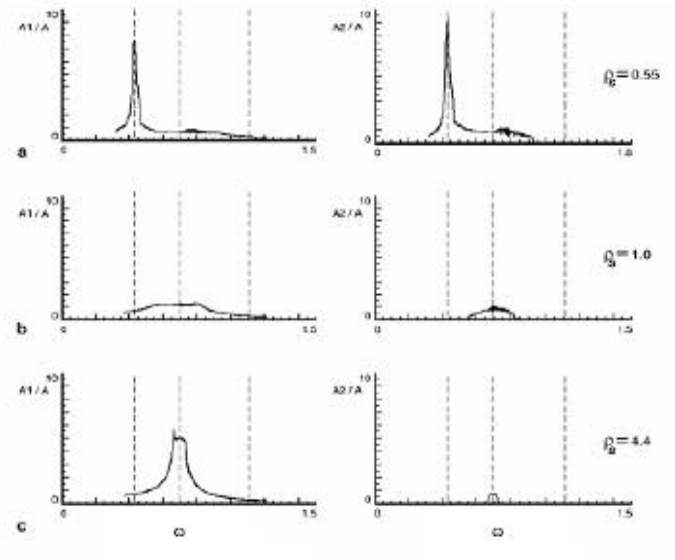

Figure 11 Measured frequency response curves (Hartung et. al.'s experiment scanned from [18])

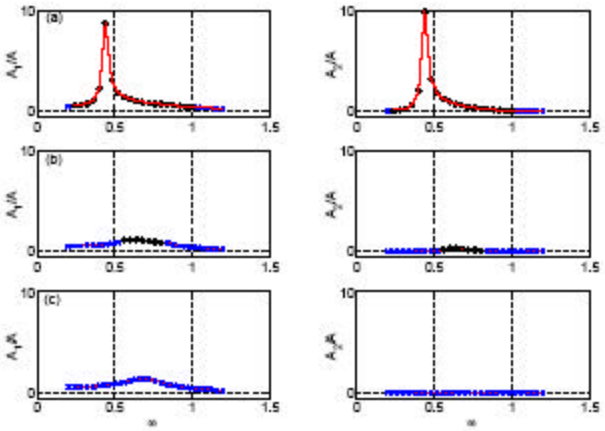

Figure 12 Simulated frequency response curves. ×××, pure stick solution; ooo, discontinuous model (stick-slip) solution; ___, smoothened friction model with σ = 50

NEGATIVE SLOPE IN FRICTION FORMULATION

Although only the case $m_s = m_k$ has been considered in this study, several previous researchers, including Karnopp [19] and Shaw [20], have suggested a general formulation where $m_k < m_s$. For example, consider the following formulation [21] where m_s has been normalized with respect to m_k (=1.0) and a is a factor that controls the exponentially decaying gradient.

$$m(\dot{d}_1) = \begin{cases} \left[1.0 + (m_s - 1.0)e^{-a|\dot{d}_1|}\right]\mathrm{sgn}(\dot{d}_1) & |\dot{d}_1| > 0 \\ [0 \quad m_s] & \dot{d}_1 = 0 \end{cases} \tag{23}$$

Further, we can condition the discontinuous formulation (23) by employing the hyperbolic-tangent function (9).

$$m(\dot{d}_1) = [1.0 + (m_s - 1.0)e^{-a|\dot{d}_1|}]\tanh(s\dot{d}_1) \tag{24a}$$

$$\frac{\partial m}{\partial \dot{d}_1} = s\,[1.0 + (m_s - 1.0)e^{-a|\dot{d}_1|}][1.0 - \tanh^2(s\dot{d}_1)] - a\,(m_s - 1.0)e^{-a|\dot{d}_1|}\,sgn(\dot{d}_1)\tanh(s\dot{d}_1) \tag{24b}$$

Note that when $m_s > 1.0$, a negative slope ($\partial m / \partial \dot{d}_1 < 0$) is found in the friction law. Although (24) is different from (9) that implicitly assumes $m_s = m_k$, the transition frequency from the pure stick state to the stick-slip regime can still be analytically determined via the procedure developed based on linear system analysis. For example, an increase in m_s will enhance the value of T_{sf} and hence yield a narrower the stick-slip frequency regime as shown previously in Figure 3b. Further, some previous researchers have shown that the resulting "negative damping" could induce dynamic instabilities into some physical systems where the friction element acts as a passive damper [20]. Further researches along this direction have been reported in Ref. [22-23] in the context of a friction path in torsional systems. For instance, Ref. [22] has shown the significance of the clutch actuation phase on judder behavior. Although the real life fiction characteristics may vary with operating conditions such as oil temperature and pressure, our analysis is believed to capture the essence of the system dynamics.

CONCLUSION

Unlike previous studies that focused on the frictional interface models, we have examined the non-linear time and frequency domain responses of a 3DOF system subjected to localized stick-slip motions. First, a procedure to calculate the stick to slip boundaries has been developed based on the linear system theory. This procedure yields reliable prediction of the thresholds and thus it can quickly identify linear or non-linear frequency regimes. Second, the effect of the secondary inertia is investigated in-depth using both time and frequency domain calculations. Both approximate analytical and numerical solutions clearly illustrate that even a very small secondary inertia has a significant influence on the behavior and thus the bi-linear friction system (such as Figure 6) must be used with caution. As evident from time histories and frequency responses, the amplitudes of $d_2(t)$ are bounded for a bi-linear system and its frequency responses form a flat top. But when $I_2 \neq 0$, no specific bounds can be defined for $d_2(t)$ and its frequency responses show resonance-like curves. These resonances are essentially determined by a combination

of 2 states: 2DOF and 3DOF non-linear system responses.

ACKNOWLEDGMENT

Research support from the DaimlerChrysler Challenge Fund is gratefully acknowledged.

REFERENCES

1. Brack, K., Beschreibung und Implementierung des Uebertragungsverhaltens von hydrodynamischen Drehmomentwandlern in MSC/NASTRAN, Diplomarbeit, Universitaet Kaiserslautern, 1996.
2. Fischer, R., and Otto, D., Torque Converter Clutch Systems, the 5th Luk Symposium, pp. 107-138, May 1994.
3. Personal discussion with DaimlerChrysler powertrain engineers in April 2002.
4. Hiramatsu, T., Akagi, T., and Yoneda, H., Control Technology of Minimal Slip-Type Torque Converter Clutch, SAE 850460.
5. Tsangarides, M.C., and Tobler, W.E., Dynamic Behavior of a Torque Converter with Centrifugal Bypass Clutch, SAE 850461.
6. Padmanabhan, C., and Singh, R., Dynamics of a Piecewise Non-Linear System Subject to Dual Harmonic Excitation Using Parametric Continuation, Journal of Sound and Vibration, Vol. 184 (5), pp. 767-799, 1995.
7. Yamada, N., and Ando, K., An Analysis of Clutch Self-Excited Vibration in Automotive Drive Line, SAE Paper 951319, 1995.
8. Dormand, J. R., and Prince, P.J., A Family of Embedded Runge-Kutta Formulae, J. Computational and Applied Mathematics, Vol. 6, No. 1, pp. 19-26, 1980.
9. Iwan, W.D., A Distributed-Element Model for Hyteresis and Its Steady-State Dynamic Response, Transaction of the ASME, Journal of Applied Mechanics, Vol. 33, pp. 893-900, December 1966.
10. Menq, C.H., Griffin, J.H. and Bielak, J., The Forced Response of Shrouded Fan Stages, Transaction of ASME, Journal of Vibration, Acoustics, Stress, and Reliability in Design, Vol. 108/51, pp. 50-55, Jan 1986.
11. Wang, J.H. and Chen, W.K., Investigation of the Vibration of a Blade with Friction Damper by HBM, Transaction of ASME, Journal of Engineering for Gas Turbines and Power, Vol. 115/295, pp. 294-299, April 1993.
12. Wang, J.H., Design of a Friction Damper to Control Vibration of Turbine Blades, Dynamics with Friction: Modeling, Analysis and Experiment, pp. 169-195, edited by Guran, A., Pfeiffer, F., and Popp, K., 1996.
13. Ferri, A. A., and Heck, B.S., Vibration Analysis of Dry Friction Damped Turbine Blades using Singular Perturbation Theory, AMD-Vol. 192/DE-Vol. 78, Nonlinear and Stochastic Dynamics, ASME, pp. 47-56, 1994.
14. Nayfeh, A.H., and Mook, D.T., Nonlinear Oscillations, John Wiley & Sons, 1995.
15. Den Hartog, J.P., Mechanical Vibrations, Dover Publications, 1985
16. Andronov, A.A., Vitt, A.A., and Khaikin, S.E., Theory of Oscillators, Dover Publications, 1987.
17. Minorsky, N., Non-linear Mechanics, J.W. Edwards, 1947.
18. Hartung, A., Schmieg H. and Vielsack, P., Passive Vibration Absorber with Dry Friction, Archive of Applied Mechanics, Vol. 71, pp. 463-472, 2001.
19. Karnopp, D., Computer Simulation of Stick-Slip Friction in Mechanical Dynamic Systems, Transaction of the ASME, Journal of Dynamic Systems, Measurement, and Control, Vol. 107, pp. 100-103, March 1985
20. Shaw, S.W., On the Dynamic Response of a System with Dry Friction, Journal of Sound and Vibration, Vol. 108(2), pp. 305-325, 1986.
21. Berger, E.J., Friction Modeling for Dynamic System Simulation, Applied Mechanics Reviews, Vol. 55(6), pp. 535-577, 2002.
22. Duan, C., and Singh, R., Transient Responses of a 2-DOF Torsional System with Nonlinear Dry Friction under a Harmonically Varying Normal Load, Journal of Sound and Vibration, 2005 (in press).
23. Duan, C., and Singh, R., Influence of Harmonically-Varying Normal Load on Steady State Behavior of a 2DOF Torsional System with Dry Friction, submitted to the Journal of Sound and Vibration, November 2004.

CONTACT

Professor Rajendra Singh
Acoustics and Dynamics Laboratory
Center for Automotive Research
The Ohio State University
Email: singh.3@osu.edu
Phone 614-292-9044
Website: www.AutoNVH.org

LIST OF SYMBOLS

C	viscous damping coefficient (N-m-s/rad)
F	force (N)
I	torsional inertia (kg-m^2)
K	torsional stiffness (N-m/rad)
m	dimensionless mass
P	period (s)
t	time (s)
T	torque (N-m)
V	relative velocity
d	relative angular displacement (radian)
q	absolute angular displacement (rad)

m	friction coefficient
s	conditioning factor
y	phase lag (rad)
Ω	angular speed (rad/s)
w	excitation frequency (rad/s)
j	phase lag (rad)
x	normalized absolute displacement
ρ	dimensionless friction force amplitude

Subscripts

1,2,3	inertial element indices
c	critical or transition
D	drag load
e	engine or equivalent
eq	equivalent
f	friction
k	kinetic
m	mean
n	natural frequency
max	maximum
min	minimum
p	fluctuating component or perturbation
s	static
sf	saturation

Superscripts

.	first derivative with respect to time
..	second derivative with respect to time